Development

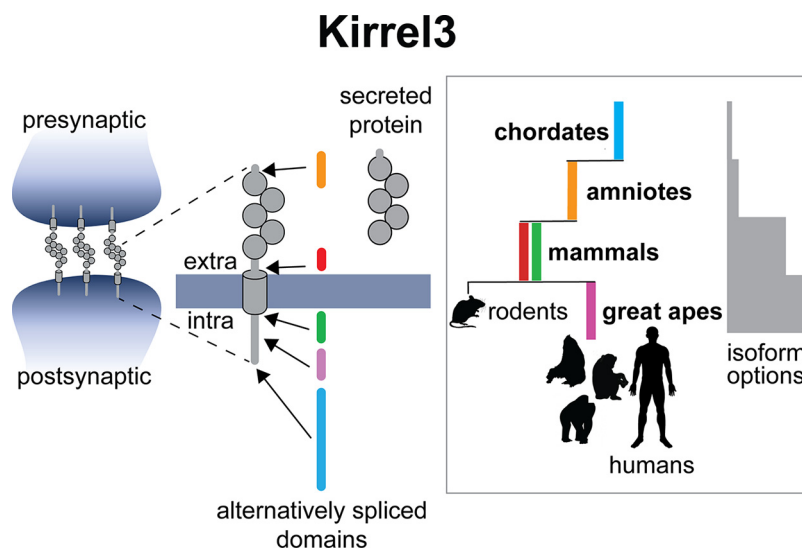# Modular Splicing Is Linked to Evolution in the Synapse-Specificity Molecule Kirrel3

Dimitri Traenkner, Omar Shennib, Alyssa Johnson, Adam Weinbrom, Matthew R. Taylor, and Megan E. Williams

https://doi.org/10.1523/ENEURO.0253-23.2023

Department of Neurobiology, University of Utah, School of Medicine, Salt Lake City, UT 84112

Visual Abstract

Abstract

Kirrel3 is a cell-adhesion molecule that instructs the formation of specific synapses during brain development in mouse and Kirrel3 variants may be risk factors for autism and intellectual disabilities in humans. Kirrel3 is predicted to undergo alternative splicing but brain isoforms have not been studied. Here, we present the first in-depth characterization of Kirrel3 isoform diversity in brain using targeted, long-read mRNA sequencing of mouse hippocampus. We identified 19 isoforms with predicted transmembrane and secreted forms and show that even rare isoforms generate detectable protein in the brain. We also analyzed publicly-available long-read

Significance Statement

Kirrel3 is an important molecule for synapse and circuit formation with gene variants that are associated with neurodevelopmental disorders, yet Kirrel3 function remains largely unknown. Here, we report new iso-forms of mouse and human Kirrel3, including secreted and transmembrane forms, that suggest a diverse repertoire of Kirrel3 actions. Importantly, we identified a new Kirrel3 exon only present in humans and the other great apes with potential to play an important role in circuit formation unique to these species.

mRNA databases from human brain tissue and found 11 Kirrel3 isoforms that, similar to mouse, encode transmembrane and secreted forms. In mice and humans, Kirrel3 diversity arises from alternative, independent use of protein-domain coding exons and alternative early translation-stop signals. Intriguingly, the alternatively spliced exons appear at branch points in the chordate phylogenetic tree, including one exon only found in humans and their closest living relatives, the great apes. Together, these results validate a simple pipeline for analyzing isoform diversity in genes with low expression and suggest that Kirrel3 function is fine-tuned by alternative splicing and may play a role in brain evolution.

Key words: alternative splicing; cell adhesion; evolution; Kirrel3; synapse

Introduction

Proper wiring of the mammalian brain requires billions of neurons to form synaptic connections with specific neurons. During development, axons extend to correct brain regions and then synapse with suitable neuronal partners, a process largely governed by the cellular environment, morphology, and cell surface proteins. Cell surface proteins help the cell find matching and avoid nonmatching synaptic partners (Sanes and Zipursky, 2020; Südhof, 2021). They also function in development by contributing to synapse formation and, likely, continue to function throughout adulthood during synapse maintenance, transmission, and plasticity.

The combinatorial expression of synaptic cell surface proteins provides different cell types with a unique identity that can be further tuned by alternative splicing. Alternative splicing of synaptic molecules can affect their protein-protein interactions and intracellular signaling (Südhof, 2017; Ovando-Zambrano et al., 2019; Li et al., 2020; Gomez et al., 2021; Trotter et al., 2023). This, in turn, expands the functional repertoire of synaptic genes and adds a layer of regulatory control. Accordingly, splicing factors are important for all aspects of neural development including neuronal health and accurate neuronal wiring (Furlanis and Scheiffele, 2018; Traunmüller et al., 2023). Despite the emerging importance and widespread use of alternative splicing programs in synaptic proteins (Ray et al., 2020), isoform diversity has been characterized for relatively few cell adhesion proteins including Dscam, Neurexin, and the Neurexin binding partners Neuroligin, Teneurin, and Latrophilin (Hattori et al., 2008; Schreiner et al., 2014; Treutlein et al., 2014; Südhof, 2017;

Ovando-Zambrano et al., 2019; Li et al., 2020; Gomez et al., 2021).

Kirrel3 is a single pass transmembrane protein in the immunoglobulin (Ig) superfamily with five extracellular Ig domains and an intracellular PDZ-binding domain. Kirrel3 mediates cell-adhesion and synapse formation via transcellular, homophilic interactions and is essential for normal brain connectivity in mice (Prince et al., 2013; Martin et al., 2015, 2017; Roh et al., 2017; Brignall et al., 2018; Taylor et al., 2020; J. Wang et al., 2021). The Kirrel3 gene is composed of many small exons predicted to undergo alternative splicing. So far, three isoforms were reported in skeletal muscle (Durcan et al., 2014), but Kirrel3 isoform diversity has not been tested in the brain. Understanding the alternative splicing program of Kirrel3 is expected to provide new insight to its function in synapse and circuit formation. In addition, understanding the alternative splicing of Kirrel3 may facilitate the study of disease mechanisms that involve this synaptic gene because human Kirrel3 missense variants have been repeatedly identified as risk factors for neurodevelopmental disorders including autism spectrum disorders and intellectual disabilities (Bhalla et al., 2008; De Rubeis et al., 2014; Iossifov et al., 2014; T. Wang et al., 2016; Yuen et al., 2016; Li et al., 2017; Kalsner et al., 2018; Guo et al., 2019; Leblond et al., 2019; Hildebrand et al., 2020; Taylor et al., 2020; Zhou et al., 2022).

Here, we generated a comprehensive list of Kirrel3 isoforms expressed in the mouse hippocampus obtained with targeted long-read mRNA sequencing. In addition, we examined existing long-read transcriptome data from multiple mouse and human brain regions. We identified a total of 19 mouse and 11 human alternative transcripts predicted to encode distinct Kirrel3 proteins including secreted and transmembrane variants. In both mice and humans, Kirrel3 isoform diversity originates in the independent combination of four protein coding exons, two on the extracellular and two on the intracellular side, together with several alternative C termini. The four alternatively spliced protein coding exons first appear at different critical branching points in the chordate phylogenetic tree. Moreover, we identified a new alternatively spliced protein-coding Kirrel3 exon exclusively present in humans and the great apes (Hominidae), suggesting a key role of Kirrel3 in regulating brain connectivity in these closely related species.

Materials and Methods

Animals

Kirrel3 knock-out (KO) mice were described previously (Prince et al., 2013) and are backcrossed to the C57Bl/6J

strain background. Male and female mice were used in equal numbers and described in the text. All animal experiments were approved and conducted in accordance with the University of Utah Institutional Animal Care and Use Committee (IACUC).

Iso-seq sample processing and analysis

RNA was purified from two whole hippocampi per sample and a total of six samples. Samples are from two C57Bl/6J P14 males and females, respectively, as well as one P14 male and female knock-out control (KO; Prince et al., 2013). RNA was tested for quality (Agilent TapeStation, RIN ≥ 8.0) and converted to cDNA (NEBNext Single Cell/Low Input RNA Library Prep kit for Illumina). cDNA from each sample was amplified and barcoded in a mild stringency PCR (20 cycles of 30 s at 98°C, 54°C and 72°C), using a target-specific forward primer matching exon 2 of mouse Kirrel3 and a universal cDNA-reverse primer (Extended Data Table 1-1). Barcoded PCR products ≥1 kb were enriched (ProNex beads) and quantified (TapeStation D5000). Equal amounts of each sample were combined into a single 500 ng SMRTbell library for full-length transcript sequencing on a single SMRTcell using the Sequel II system (Pacific Bio). Iso-seq analysis was performed using R and the R-package BioStrings (Lifschitz et al., 2022). Results were manually confirmed and aligned using ApE plasmid editor software (Davis and Jorgensen, 2022). In brief, Iso-seq reads were demultiplexed using unique 16-bp bar code sequences and no more than two mismatches as search pattern. This strategy unambiguously identified the sample origin for 85.8% of all reads. Preliminary inspection of Iso-seq Kirrel3 transcripts was performed by dividing the Kirrel3 gene (NCBI Gene ID: 67703, 550,823 bp) into 155-bp fragments, and screening Iso-seq full-length reads for the presence of any of the 3536 resulting fragments. The preliminary inspection revealed one new exon and seven new exon extensions for a total of 29 alternatively spliced genomic segments (Extended Data Table 2-1). Iso-seq reads with sample IDs were screened for each of these 29 segments with no more than 40% mismatches.

Sequence Read Archive (SRA) and phylogenetic analysis

Published mouse or human PacBio SMRT transcript libraries generated with brain derived tissues or cell lines were screened for Kirrel3 transcripts using the conserved exon 2 sequence and the NCBI blastn suite (Altschul et al., 1990). Similar to the analysis of mouse transcripts, human Kirrel3 transcripts were first inspected for the presence of any of 3772 elements, each 155 bp in length, that make up the human Kirrel3 gene (NCBI Gene ID: 84623, 584,513 bp). The preliminary inspection revealed three new exons and one new exon extension for a total of 27 alternatively spliced genomic segments (Extended Data Table 2-1). Similar to the Iso-seq analyses, mouse and human Kirrel3 transcripts were then examined for the presence of the respective alternatively spliced segments (≤40% mismatches) and manually aligned using BioStrings and ApE plasmid editor software, respectively. Phylogenetic

analyses of mouse exons 6, 18, 19b, and 22 and human exons 3, 16, 17c, 19a, and 21 were performed by comparing nucleotide sequences to published genomes using the blastn suite (Altschul et al., 1990), direct gene ortholog inspection and by examining relationship of species with matches using the NCBI Taxonomy database (Schoch et al., 2020).

Fluorescent *in situ* hybridization chain reaction (HCR)

HCR was performed as previously described (Trivedi et al., 2018). Mouse brains were cryo-sectioned to 30-μm slices, mounted on slides, fixed [4% paraformaldehyde (PFA)] and washed in PBS. Before processing samples according to protocol HCR v3.0 (Invitrogen), slices were treated with 1 μg/ml proteinase K-treated (TE buffer) and equilibrated in SSC buffer. Custom HCR probes were designed and generated by Molecular Instruments based on provided targets (Extended Data Table 4-1). After nuclear staining with Hoechst in PBS, coverslips were mounted in Fluoromount-G (Southern Biotech catalog #0100-01) and imaged (Zeiss LSM 710).

Immunoblotting

Immunoblotting was conducted by standard techniques. Mouse samples are hippocampi from a three-week-old Kirrel3 wild-type or knock-out animals. Human samples are derived from deidentified postmortem dorsolateral prefrontal cortex stored at −80°C (kindly provided by Hilary Coon). Tissue samples are from one female (21 years, post mortem interval: 11.2 h) and one male (23 years, post mortem interval: 11.6 h). Mouse and human samples were processed in a Dounce homogenizer in lysis buffer (50 mM Tris, pH 7.5, 150 mM NaCl, 5 mM EDTA, 10% Glycerol, 1% CHAPS) with protease inhibitors at 100 mg/ml. The lysate was boiled in Laemmli buffer, run in a 10% bis-tris gel, and transferred to a nitrocellulose membrane. Antibodies used included mouse-anti-Pan-Kirrel3 (Neuromab, RRID: AB_2315857), mouse anti-Kirrel3[exon19b] (Neuromab, RRID: AB_2341106), mouse-anti-GAPDH (Millipore, catalog #AB2302, RRID: AB_10615768), and a custom rabbit anti-Kirrel3 made against a C-terminal peptide (Martin et al., 2015). Secondary antibodies were goat-anti-mouse-HRP (Jackson ImmunoResearch, catalog #115-035-003, RRID: AB_10015289) and goat-anti-rabbit-HRP (Jackson ImmunoResearch, catalog #111-036-003, RRID: AB_2337942).

DNA constructs

cDNAs and plasmids were generated using standard PCR-based restriction enzyme cloning (Taylor et al., 2020). Extracellular FLAG tags were added to mouse Kirrel3 Isoforms F (Kirrel3F) and K (Kirrel3K) in frame after the predicted signal-peptide cleavage site (exon 6) and the tagged constructs placed 3′ to mCherry or GFP followed by a viral 2A peptide sequence into the mammalian expression vector pBOS (mCherry-2A-FLAG-Kirrel3F/K).

Cell aggregation assay

CHO cells were transfected with either mCherry-2A-FLAG-Kirrel3F, mCherry-2A-FLAG-Kirrel3K, GFP-2A-FLAG-

Kirrel3F, or pBOS with mCherry only (mCherry-pBOS). After 48 h, transfected cells were washed and detached (0.01% trypsin) in magnesium-free HEPES buffer (HMF; 137 mM NaCl, 5.4 mM KCl, 1 mM CaCl2, 0.34 mM Na$_2$HPO$_4$, 5.6 mM glucose, and 10 mM HEPES, pH 7.4), spun down, and resuspended in HMF. Next, 100 000 cells suspended in 0.5 ml HMF were allowed to aggregate for 90 min (nutator, 37°C) in BSA-coated 24-well plates. For analysis, cells are fixed by adding paraformaldehyde (PFA; 4% final) and allowed to settle over a 24-h period. All but 0.3 ml of the supernatant are removed, cells and cell aggregates are carefully transferred in the remaining volume to a 96-well glass bottom plate, and the entire well is imaged (Zeiss LSM 710). Finally, the fraction of aggregated cells in the entire well was determined using ImageJ software.

Immunocytochemistry and analysis

293T-HEK cells on poly-D-Lysine treated glass coverslips were transfected using PEI following a previously published protocol (Xie et al., 2013). After 24 h, cells were fixed (4% PFA) and rinsed with PBS and blocked for 30 min with 3% BSA/0.1% Triton X-100 in PBS (blocking buffer). Blocking buffer was also used for all subsequent washes and antibody dilutions. For antigen labeling, cells were incubated for 1–2 h with primary antibody at room temperature, washed three times, and incubated for 45 min with secondary antibody. After nuclear staining with Hoechst in PBS, coverslips were mounted in Fluoromount-G and imaged (Zeiss LSM 710). The relative enrichment of membrane proteins in cell-to-cell contacts was measured as ratio of average fluorescence pixel intensity along a cell's contact versus free membrane using ImageJ software.

Statistics

For the CHO aggregation experiment, the sample size ($n = 3$ for all conditions) indicates independent experiments conducted on different days. Groups were compared by a one-way ANOVA followed by pair-wise post-tests. For the cell junctional enrichment assay, we sampled several cells from three independent cultures and used a nested one-way ANOVA followed by pair-wise post-tests.

Availability of data and materials

Iso-seq sequencing data are available at NCBI under SRA data file number PRJNA992104. Kirrel3 isoform sequence files have been deposited at NCBI. GenBank accession numbers for mouse Kirrel3 mRNA Isoforms F–T are OR239801–OR239815, respectively. All other materials and data that are not commercially available will be freely provided on reasonable request.

Results

A strategy to enrich for full-length Kirrel3 transcripts

Commonly used deep-sequencing technologies rely on short sequence reads (<250 bp) that are powerful assets in defining whole cell or tissue transcriptomes (Corchete et al., 2020). Short sequence reads are suitable to determine relative transcript frequencies and relative exon

usage for all genes expressed. However, short-read sequencing is not suitable to directly determine the complete exon composition of transcripts longer than the 250-bp read limit (Leshkowitz et al., 2022). Recent advances in long-sequence read technologies such as Iso-seq (Kuo et al., 2017) or Nanopore sequencing (Y. Wang et al., 2021) can generate millions of high-quality reads of >15 kb that allow full-length transcript characterization. To capture full-length Kirrel3 transcripts, we performed Iso-seq experiments on RNA collected from hippocampal tissue from 14-d-old C57Bl/6J mice ($n = 4$, 2 males, and 2 females). As a synapse specificity molecule, Kirrel3 is not an abundant transcript nor protein. Based on published RNA sequencing data on mouse brain samples (Bioproject PRJDB7898, five replicates), we estimate that Kirrel3 transcripts comprise an extremely small proportion of the overall mRNA content (<0.001%). Therefore, before conducting long-read sequencing, we enriched libraries for Kirrel3 transcripts. We accomplished this via a PCR amplification step using a forward primer matching exon 2 of Kirrel3 and a universal reverse primer with the sequence AAGCAGTGGTATCAACGCAGAGT, which was originally ligated to all transcripts during cDNA synthesis (Fig. 1). In addition, a unique Iso-seq library bar code was added to each sample in this step to allow for simultaneous sequencing of all samples in a single sequencing run. We chose the target-specific primer because exon 2 contains the start codon required for all known and predicted Kirrel3 isoforms. We also conducted Iso-seq on samples from 14-d-old male and female Kirrel3 knock-out mice (Prince et al., 2013) as sequencing and data analyses controls. We find that our modified Iso-seq strategy using a Kirrel3-specific primer generated datasets with a total of 1,394,974 reads including 11,328 Kirrel3 reads (0.8%). Although Kirrel3 remains a small part of the total dataset, we estimate that Kirrel3 transcripts were enriched over 1600-fold on average compared with whole-transcriptome libraries from brain tissue.

Four independently spliced exons and alternative C termini generate a diversity of Kirrel3 transcripts

In our custom analysis pipeline, 85.8% of transcript reads could be assigned to a sample based on sample-specific barcodes (Fig. 1; Extended Data Table 1-1). The remaining 14.2% of all transcripts either contained incomplete or no bar code and were excluded from subsequent analyses. To uncover new Kirrel3 exons, we screened transcripts of each sample for the presence of any known Kirrel3 sequence, including predicted intron sequences (NCBI Gene ID: 67703). Consistent with our PCR strategy to enrich for Kirrel3 transcripts beginning at exon 2, exon 1 of Kirrel3 was absent in our Iso-seq dataset. Moreover, hippocampal Kirrel3 transcripts neither contained predicted exons 3 and 4 (ENSEMBL genome browser, ENSMUSG00000032036), nor previously published exon 5, but we included them in the overall gene structure shown in Figure 2A for completeness (Fig. 2A, dashed boxes). Analysis of Kirrel3 transcripts indicates a total of 22 exons, one of which was not previously reported (exon 10 in Fig. 2A). These exons are alternatively spliced to generate 19 distinct
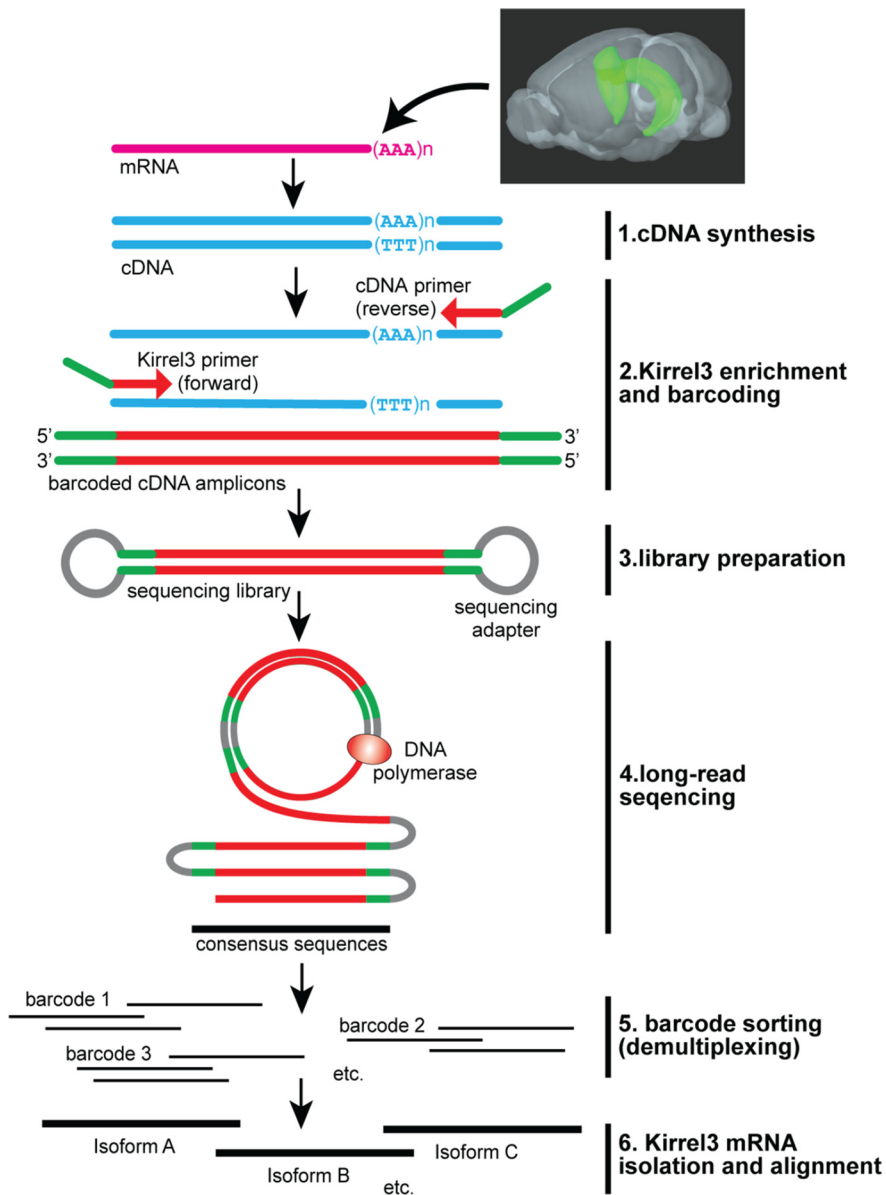
Figure 1. Long-read transcript sequencing. Schematic of the long-read sequencing workflow starting with total mRNA from P14 hippocampal tissue. Pink indicates mRNA, blue cDNA, green DNA-barcodes, red raw Kirrel3 sequences, gray sequencing adapters, and black consensus Kirrel3 sequences. Extended Data Table 1-1 reports the sequence of each bar code used.

isoforms in mouse hippocampus. Five were previously identified and designated as Isoforms A–E. Using the same logic, new isoforms are identified with a letter (Fig. 2B,C). Based on our data, we also estimated the frequency of each isoform (Fig. 2A,B) and the cumulative frequency of each predicted protein domain (Fig. 2D).

Kirrel3 exons found in hippocampal transcripts fall into three groups. The first group contains constitutive exons present in all isoforms found in the hippocampus (Fig. 2A–C, gray boxes). The second group are exons that are either fully included or skipped (exons 6, 18, 22). Exon 6 contains a signal-peptide cleavage site and is present in most transcripts. If exon 6 is skipped, an alternative signal peptide is predicted. As a consequence, slightly different extracellular N termini are generated dependent on the

presence or absence of exon 6. The third group of exons (8, 9, 11, 13, 17, 19, and 20) are found in transcripts with either extended or nonextended 3′ ends, suggesting that they contain two alternative 3′ splice sites (Xia et al., 2006; Keren et al., 2010; Suñé-Pou et al., 2017). In Figure 2, segments that extend an exon are labeled with the letter "b," the respective nonextended exons are labeled with "a." If included in the transcript, six out of the seven b segments (8b, 9b, 11b, 13b, 17b, and 20b) introduce a stop-codon (Fig. 2A–C, white boxes) and produce an alternative C terminus in the Kirrel3 protein. Exons 8b, 9b, 11b, 13b, 17b, and the newly identified exon 10 (Fig. 2A, asterisks) are predicted to generate secreted proteins with different numbers of Ig-domains (Fig. 2D). In contrast, exon 20b is predicted
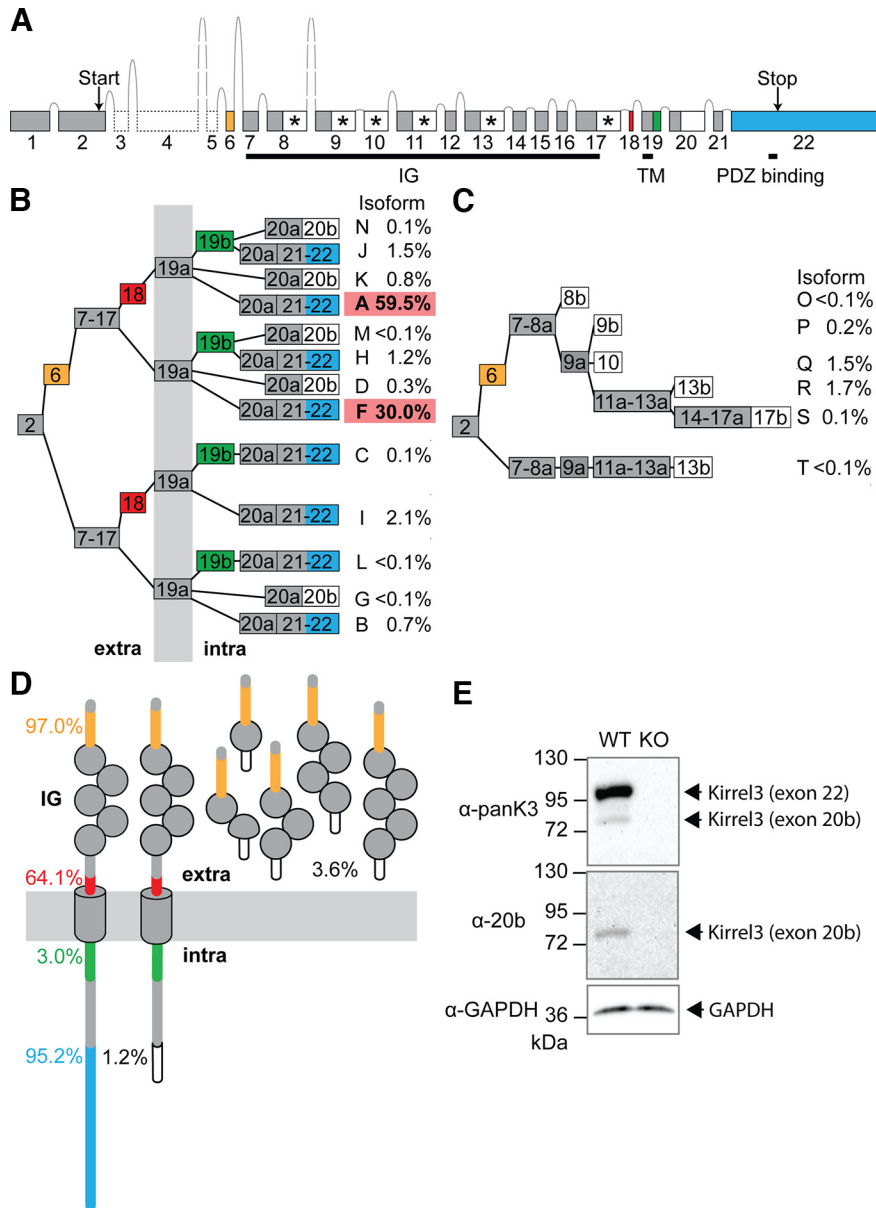
Figure 2. Mouse Kirrel3 gene, transcript isoforms, and proteins. *A*, Genomic organization of the mouse Kirrel3 gene, with exons (boxes) and introns (lines), including four independently spliced protein-coding exons (yellow, red, green, and blue). White boxes mark exons or exon parts with a stop-codon. Exons producing predicted secreted Kirrel3 isoforms are additionally marked with an asterisk. *B*, Alternative splicing of Kirrel3 exons is predicted to produce 13 different transmembrane isoforms. Isoforms are given letters, following the example of previously identified Isoforms A–E. Isoform E, the only transcript including exon 5, was not identified in the hippocampus. Exons 8, 9, 11, 13, 17, 19, and 20 are present in transcripts as short (part a) or extended (parts a + b) versions. Percent indicate the relative contribution of a particular Kirrel3 isoform to the total number of complete Kirrel3-transcripts featuring exon 2 and poly A-tail. Exons encode protein segments that are either extracellular ("extra"), intracellular ("intra"), or spanning the membrane (gray vertical bar). *C*, Six predicted secreted Kirrel3 isoforms (O–T) only comprise extracellular domains. *D*, Schematic of Kirrel3 protein isoforms. Percent are estimates of how frequent protein domains are present in hippocampal Kirrel3 based on isoform frequencies. *E*, Western immunoblots from hippocampi from three-week-old wild-type and Kirrel3 knock-out mice using antibodies directed against Kirrel3 amino acids 46–524 (αpanK3), the peptide encoded by exon 20b (α–20b), or house-keeping gene glyceraldehyde 3-phosphate dehydrogenase (αGAPDH). IG: Ig-domain, TM: transmembrane domain. Extended Data Table 2-1 reports the exact sequences for each mouse and human exon as well as SRA files.

to generate a transmembrane protein with a short intracellular domain lacking the Kirrel3 PDZ-binding domain. Exon 19b does not produce a protein stop, but codes for 25 additional amino acids just intracellular to the transmembrane domain.

The vast majority of isoforms (95%) contain exon 22 and, thus, encode transmembrane proteins with a C-terminal PDZ-binding domain. In contrast, the alternatively generated transmembrane protein with a short intracellular domain lacking a PDZ-binding domain is found in just over 1% of all

transcripts. Together with exons 6, 18, and 19b, exon 22 is one of four alternatively spliced exons that appear to be included or excluded from Kirrel3 transcripts independent from each other.

We confirmed our findings by searching published Iso-seq transcript libraries for mouse hippocampus and other brain regions. We found a total of 2237 Kirrel3 transcripts distributed across 21 published mouse Iso-seq libraries (Extended Data Table 2-1) but did not detect additional isoforms. Finally, samples from Kirrel3 knock-out mouse controls produced the expected 5′ untranslated region (UTR) of exon 2 followed by an eGFP coding sequence, which is consistent with how these germline knock-out mice were constructed (Prince et al., 2013).

Different Kirrel3 protein isoforms are found in brain tissue

Next, we tested whether we could identify distinct Kirrel3-protein isoforms in brain tissue. We initially focused on the existence of isoforms with different intracellular domains because the predicted proteins can be easily resolved by size on a Western blotting. We used a pan-Kirrel3 antibody against the extracellular domain and an isoform-specific antibody that selectively recognizes isoforms containing the short intracellular domain caused by inclusion of exon 20b. We examined immunoblots of mouse hippocampal lysates using the pan-Kirrel3 antibody and detected two bands that run at the expected molecular weight for full length proteins with the long and short intracellular domains (Fig. 2E) in wild-type but not Kirrel3 KO tissue. We then blotted the same lysates using the antibody specific to the short intracellular domain only and observed a single band at the lower molecular weight. The results of the immunoblot demonstrate that distinct Kirrel3 isoforms can be identified in brain tissue and that both exon 20b and exon 22 containing mRNA isoforms give rise to proteins in the brain.

Exons 18, 20b, and 22 do not directly affect Kirrel3-mediated homophilic cell adhesion

Homophilic, transcellular binding is necessary for Kirrel3-mediated synapse formation (Taylor et al., 2020) and structural studies indicate that Kirrel3-Kirrel3 trans binding is mediated predominantly by its first, most N-terminal Ig-domain (J. Wang et al., 2021). However, accumulating evidence suggests that intracellular domains can allosterically alter the ligand-binding properties of extracellular domains, either directly by inducing conformation changes, indirectly via additional factors, or by altering the stoichiometric assembly of transmembrane receptors (Changeux and Christopoulos, 2017; Ortiz Zacarías et al., 2018; X. Wang et al., 2018; Lara et al., 2019). Moreover, a disease-associated missense variant in the intracellular domain was recently identified that significantly attenuates Kirrel3 trans-cellular binding (Taylor et al., 2020). Thus, we wondered whether the C-terminus choice of Kirrel3 affects homophilic cell-adhesion using an established *in vitro* cell aggregation assay. To test this, we generated expression plasmids encoding cDNAs

for isoforms that contain exon 22 (Isoform F) or 20b (Isoform K; Fig. 2B). By comparing Isoforms F and K, we sought to also obtain information about whether the selectively spliced extracellular domain encoded by exon 18 affects the homophilic transcellular binding of Kirrel3. Exon 18 is present in Isoform K, but not in Isoform F. We found that suspended cells expressing either Kirrel3 Isoform F or K readily form homophilic and heterophilic aggregates, but control cells expressing mCherry do not (Fig. 3A,B; Extended Data Table 3-1). We also find that cells co-expressing Isoforms F and K aggregate (Fig. 3A, B; Extended Data Table 3-1). Similarly, both Kirrel3 isoforms are significantly enriched at cell-cell junctional membranes as compared with other membrane regions when both contacting cells express Kirrel3 (Fig. 3C–G; Extended Data Table 3-1). In contrast, neither membrane-GFP nor Neuroligin (a transmembrane protein that does not undergo homophilic binding in trans) are enriched at cell-cell junctional membranes as compared with other membranes (Fig. 3C–G). Of note, we confirmed that neither HEK293 nor CHO cells used in any of these assays endogenously express detectable levels of Kirrel3 protein (Extended Data Fig. 3-1). Together, these results show that Kirrel3 Isoforms F and K undergo homophilic transcellular binding and suggest that the inclusion or exclusion of exons 18, 20b, and 22 does not directly affect the ability of Kirrel3 to bind itself in trans.

Kirrel3 isoforms are co-expressed *in situ*

Next, we sought to test whether different cell types or even individual cells express different Kirrel3 isoforms using fluorescent mRNA *in situ* hybridization (FISH). Because Kirrel3 is not an abundant transcript and most of the alternatively spliced exons are very short, we again focused on the two longest alternatively spliced regions, which encode the alternative intracellular domains exon 22 and 20b. We generated hybridization chain reaction (HCR) FISH probes (Choi et al., 2018) selective to exons 22 and 20b and conducted FISH on brain sections of P14 wild-type and Kirrel3 knock-out tissue (Fig. 4; Extended Data Table 4-1). Consistent with previous reports (Lein et al., 2007; Taylor et al., 2020; Hisaoka et al., 2021), we find that Kirrel3 is expressed specifically by DG neurons and GABA neurons in the hippocampus. It is also expressed by many cells in the lateral posterior nucleus (LPN) of the thalamus (Fig. 4). As predicted by our sequencing results, exon 20b is less abundant than exon 22, but we did not observe obvious differences in the expression pattern of both alternatively spliced exons. When we used both probes simultaneously, we found that individual DG and GABA neurons often co-express both isoforms (Fig. 4I,J). FISH probes to smaller exons did not yield any obvious signal. This is likely a technical issue because Kirrel3 transcripts are not highly expressed and the specific probes are very short. Nonetheless, these findings argue against a cell type-specific use of alternative intracellular domains and suggests that most neurons express a mixture of Kirrel3 isoforms with and without a PDZ-binding domain.
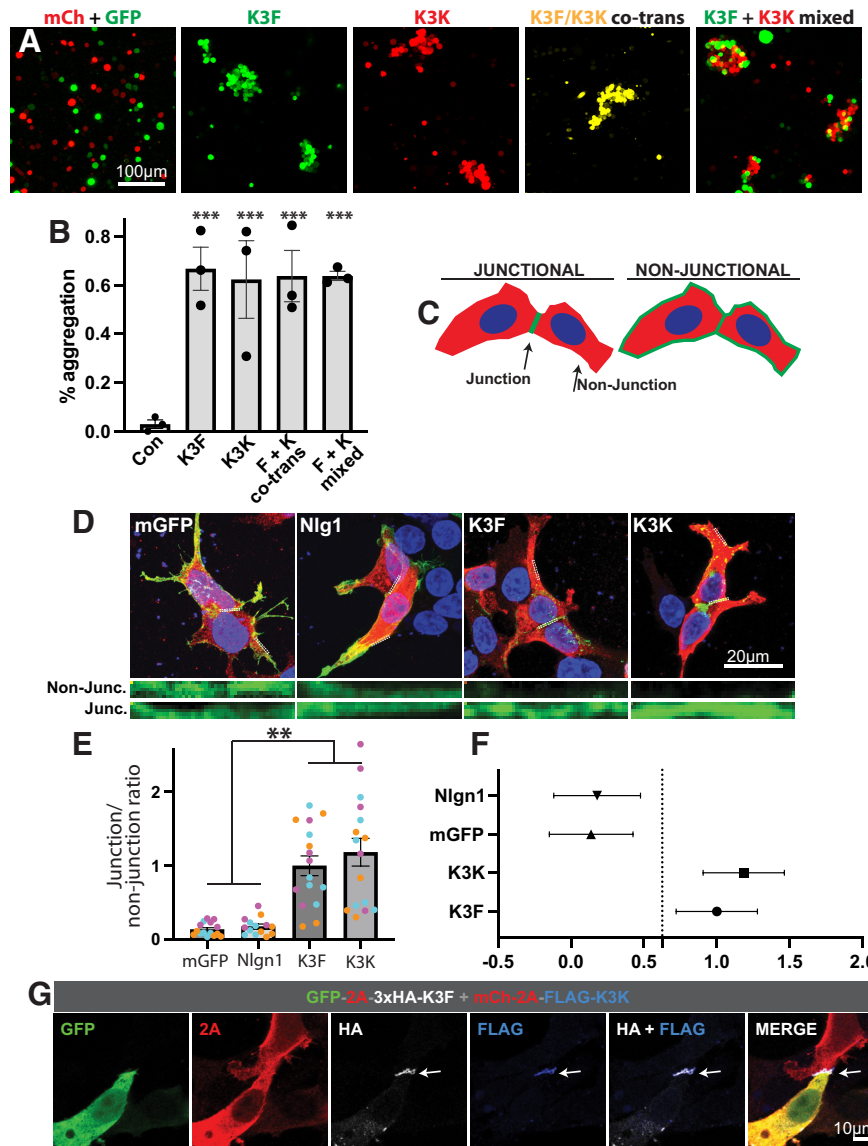
Figure 3. Homophilic binding of Kirrel3 isoforms. **A**, Example of the CHO-cell aggregation assay. CHO cells are expressing mCherry (mCh) or GFP as a control, GFP-2A-Kirrel3F (K3F), mCherry-2A-Kirrel3K (K3K) or both Kirrel3 isoforms. **B**, Quantification of CHO cell aggregation assays. $N = 3$ independent trials for each condition. Error bars = SEM $p = 0.003$ for a one-way ANOVA and ***$p < 0.001$ for each pairwise post-test comparison with the control condition. **C**, Diagram of the cell junction assay in adherent HEK293 cells. **D**, Example of the cell junction assay. Note that Kirrel3F and Kirrel3K are both highly enriched in the cell-cell junction, but the control proteins, membrane bound GFP (mGFP) and Neuroligin-1 (Nlg1), are not. **E**, **F**, Quantification of the adherent cell junction assay. **E**, Bar graphs and error bars indicate SEM. Each dot indicates a cell and each color denotes cells from an independent culture. One-way nested ANOVA indicates $p < 0.001$ and **$p < 0.01$ from pairwise post-tests. **F**, Same data but graphed as a mean estimation plot with error bars showing SD, indicating that Nlg1 and mGFP are significantly different from Kirrel3F and Kirrel3K. **G**, Example image showing that K3F and K3K cluster heterophilically in junctions when they are expressed in different cells.

The use of independently spliced Kirrel3 modules is expanded in Hominidae

To examine the extent to which our findings for mouse Kirrel3 isoforms apply to humans, we searched publicly available human brain Iso-seq libraries for reads containing Kirrel3 exon 2 (ENSEMBL genome browser, ENSG00000149571) and identified a total of 1365 transcripts distributed across 19 published libraries. Similar to our strategy for mouse, we screened the identified transcripts for the presence of any Kirrel3 gene sequence (NCBI Gene ID: 84623), including predicted intron sequences. The screen revealed three human Kirrel3 exons and one exon extension not previously reported (Fig. 5A). The human Kirrel3 gene has 21 exons and five alternative C termini, appears slightly more compact than that of the mouse, and does not contain any exons with homology to predicted mouse exons 3–5. Nevertheless, humans have orthologues to the four alternatively spliced mouse Kirrel3 protein coding exons (Fig. 5A,B). This includes an alternative signal peptide, insertions just before and after the transmembrane domain,
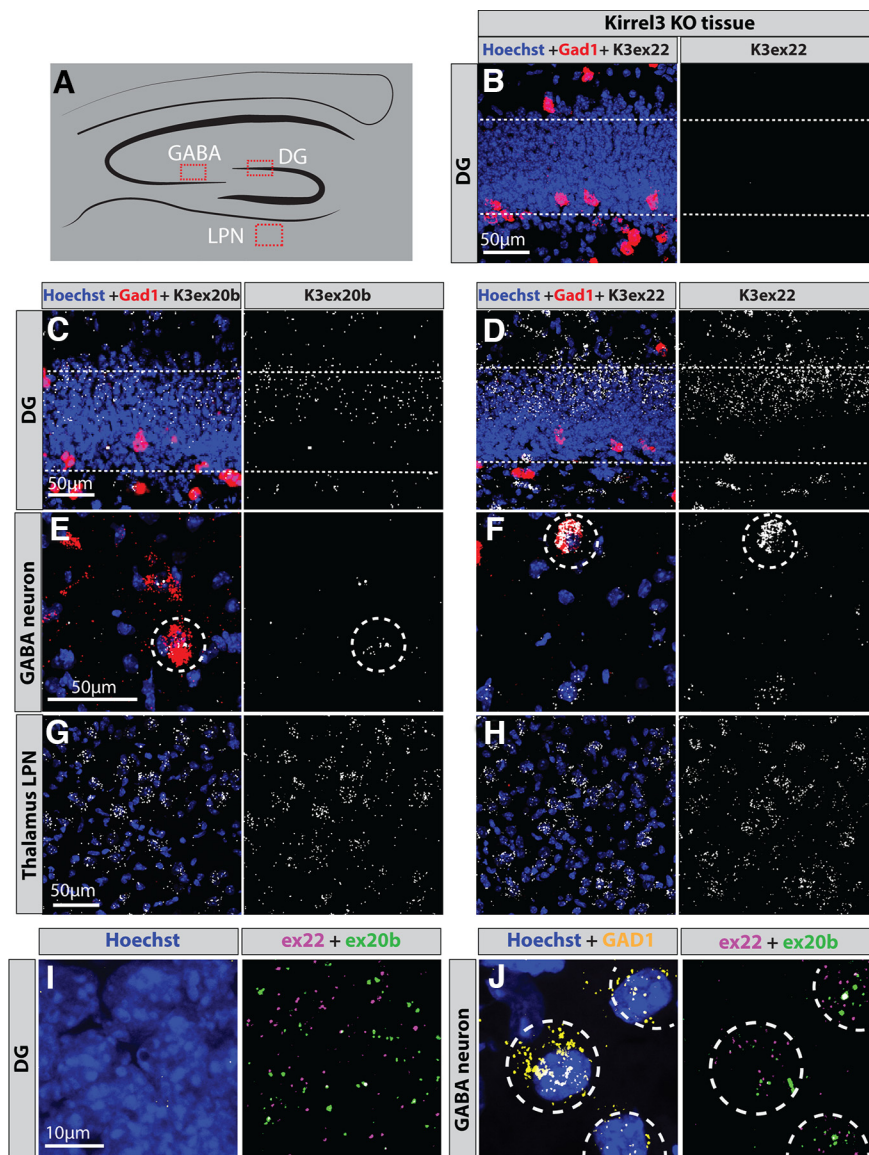
Figure 4. *In situ* detection of exons 20b and 22. **A**, Schematic of a coronal section through the hippocampus. Red boxes mark areas imaged in B-H. DG; dentate gyrus, LPN; lateral posterior nucleus of thalamus. **B–H**, Magnified images of regions shown in **A** that were hybridized with mRNA *in situ* probes for GAD1 (red) to mark GABAergic neurons, Kirrel3 exon 22 or 20b (white) as indicated to mark specific Kirrel3 isoforms, and the nuclear stain Hoechst (blue). **B**, Kirrel3 knock-out tissue produces no Kirrel3 mRNA signal using the larger exon 22 probe. **C**, **D**, Exon 22 and 20b transcripts are detected in DG neurons of wild-type mice. **E**, **F**, Exon 22 and 20b transcripts are detected in GABAergic neurons (white circles) in area CA3 of wild-type mice. **G**, **H**, Exon 22 and 20b transcripts are detected in the LPN of wild-type mice. **I**, **J**, Simultaneous use of probes for exon 22 and 20b indicate that individual neurons often express both isoforms. Extended Data Table 4-1 reports the HCR probe sets used.

and a short intracellular domain that lacks a PDZ-binding domain. Humans also have Kirrel3 isoforms with a completely new insertion (exon 19a) that adds 30 unique amino acids to the intracellular domain. Intriguingly, across all sequenced genomes a homolog to exon 19a was found only in other great apes (including chimpanzees, orangutans, and gorillas), both based on nucleotide and amino acid sequence. Moreover, our search revealed a total of 9 human Kirrel3 transcript isoforms predicted to encode different proteins, including three forms of secreted Kirrel3 (Fig. 5B, C). The transcript isoforms are designated with a number following the nomenclature of the previously identified

isoforms 1–3. Because Kirrel3 transcripts are relatively rare, it is likely that more human isoforms can be found in the future with deeper and targeted sequencing. Nonetheless, we probed lysates prepared from postmortem human prefrontal cortex tissue with an anti-Kirrel3 antibody that recognizes the longest form of Kirrel3 and find evidence that the protein is expressed in human brain (Fig. 5D).

Kirrel3 variants may be risk factors for autism spectrum disorder and intellectual disabilities in humans and we wondered whether identified disease-associated variants are located in specific exons or protein coding domains.
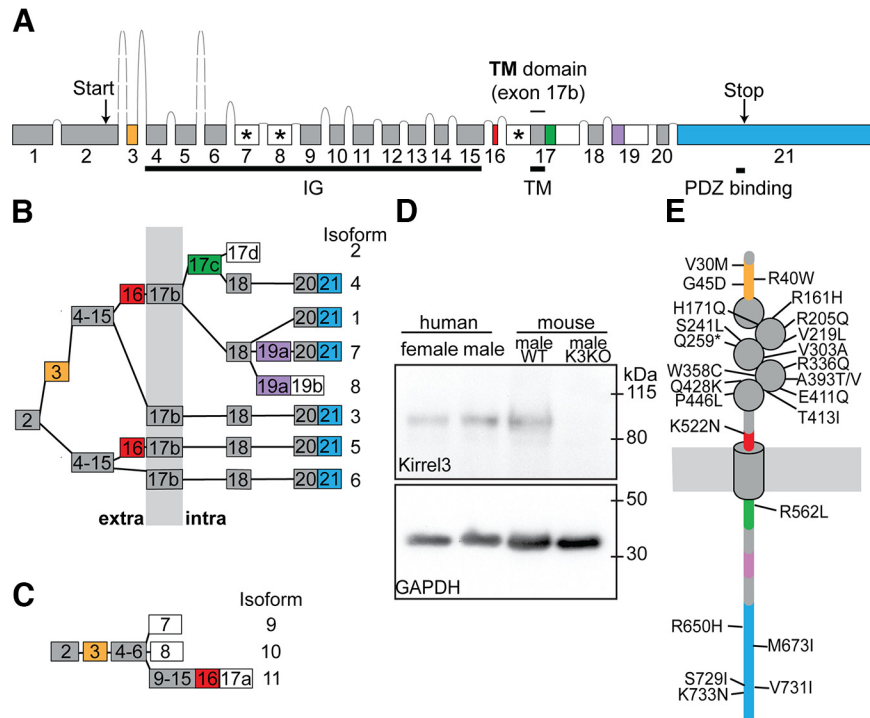
Figure 5. Human Kirrel3 gene, transcript isoforms, and proteins. **A**, Genomic organization of the human Kirrel3 gene, with exons (boxes) and introns (lines), including five independently spliced protein-coding exons (yellow, red, green, purple, and blue). White boxes mark exons or exon parts with a stop-codon. Exons producing predicted secreted Kirrel3 isoforms are additionally marked with an asterisk. **B**, Alternative splicing of Kirrel3 exons is predicted to produce eight different transmembrane isoforms. Isoforms are given numbers, following the example of previously identified isoforms 1–3. White boxes indicate exons or exon parts with stop-codon. Exons encode protein segments that are either extracellular ("extra"), intracellular ("intra"), or spanning the membrane (gray vertical bar). **C**, Three predicted secreted Kirrel3 isoforms (9–11) only comprise extracellular domains. **D**, Western blot showing that Kirrel3 protein containing human exon 21 is found in brain lysates prepared from male and female postmortem tissue (see methods). Mouse wildtype (WT) and knockout (KO) lysates are used as a positive and negative control. **E**, Schematic of Kirrel3 proteins with the position of protein domains relative to the membrane (horizontal gray bar) and mutations associated with autism. IG: Ig-domain, TM: transmembrane domain.

We searched the SFARI database (Banerjee-Basu and Packer, 2010; Abrahams et al., 2013) and the literature for Kirrel3 missense mutations associated with autism or intellectual disabilities (Bhalla et al., 2008; De Rubeis et al., 2014; Iossifov et al., 2014; T. Wang et al., 2016; Yuen et al., 2016; Li et al., 2017; Kalsner et al., 2018; Guo et al., 2019; Leblond et al., 2019; Hildebrand et al., 2020; Taylor et al., 2020; Zhou et al., 2022). Out of the 25 mutations with the strongest predicted association to disease (Fig. 5E), the majority (15) are within the Kirrel3 Ig-domains 2–5. Interestingly, no mutation with a strong disease link was found in the N-terminal Ig-domain despite its prominent role in homophilic transcellular binding. The remaining mutations are found in one of the alternatively spliced protein modules coded by exon 3 (three mutations), exons 16 and 17c (one mutation each), and exon 21 (five mutations), suggesting important roles for these exons in Kirrel3 function.

Independently spliced Kirrel3 modules appear at branch points in the chordate phylogenetic tree

Inspired by the identification of an alternatively spliced Kirrel3 exon only present in humans and their closest living relatives, we examined the presence of all five alternatively spliced protein coding Kirrel3 segments using both

nucleotide and amino acid-based searches across all published genomes. PDZ-binding domain coding exon 22 of mice first appears in combination with the Ig-domains characteristic for Kirrel3 in chordates that evolved over 500
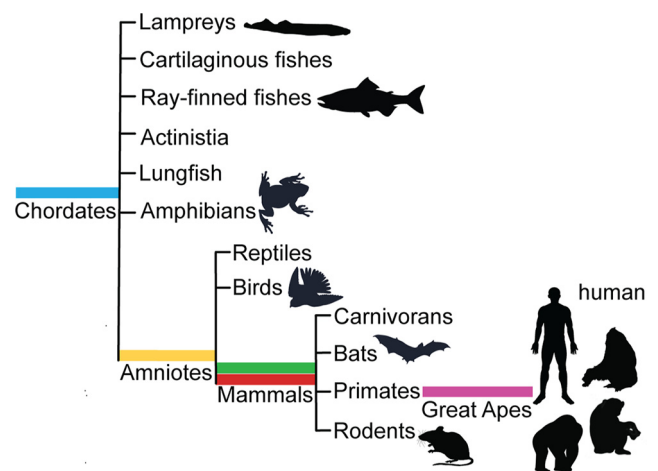

Figure 6. Phylogenetic tree of Kirrel3. The independently spliced protein-coding exons (yellow, red, green, purple, and blue as indicated in figure 5) that produce the Kirrel3 isoform variety first appear at branching points in chordate evolution.

million years ago (Holland, 2005; Fig. 6). Mouse exon 6, coding for the Kirrel3 N terminus with a cleavable signal peptide first appears in amniotes, a clade that marks the transition of tetrapods from aquatic to terrestrial habitats ∼300 million years ago (Benton and Donoghue, 2007). Mouse exons 18 and 19b, both encoding protein segments in juxtaposition to the transmembrane domain, first appear together in placental mammals which evolved in the late cretaceous around 90 million years ago (O'Leary et al., 2013). Finally, human exon 19a and its orthologues appear to be the latest addition to Kirrel3 ∼12–16 million years ago when the last common ancestor of all great apes lived (Chen and Li, 2001).

Discussion

Here, we detect an extensive repertoire of Kirrel3 mRNA isoforms in the mouse brain using a modified long-read sequencing strategy that substantially enriched Kirrel3 transcripts in the dataset. Gene-specific enrichment was an essential prerequisite to discover the extensive alternative splicing of Kirrel3, because expression of this target recognition molecule is inherently sparse and is often limited to a subset of cell types within a tissue. Consequently, we find that bulk and single cell sequencing datasets generally contain limited reads of Kirrel3 transcripts. Moreover, sequencing full-length transcripts was necessary because classic next generation sequencing generates only short reads that identify single or few exons, but not complete exon contigs. The use of long-read sequencing is particularly important for transcripts arising from exon-rich genes like Kirrel3 which features more than twice the exon count of the average gene in both mouse and human (Sakharkar et al., 2004). Because of the relatively high Kirrel3 exon count, it is not surprising that Kirrel3 isoform diversity arises from many different types of splicing events including, exon skipping, alternative 3′ exon splicing (mouse and human), and alternative 5′ exon splicing (human). These three forms of alternative splicing occur at frequencies for Kirrel3 that roughly match the proportions typical for mammalian splice events (38% exon skipping, 18% alternative 3′ splicing, 8% alternative 5′ splicing; Koren et al., 2007).

Importantly, we provide evidence that even rare Kirrel3 isoforms present in our full-length transcript dataset make detectable levels of mRNA and protein in the mouse brain. For example, exon 20b is present in only ∼1% of Kirrel3 transcripts, yet we can detect both the corresponding mRNA and protein in brain tissue using a selective in situ probe and antibody, respectively. Moreover, we demonstrate that exon 20b-containing transcripts give rise to proteins. Inclusion of exon 20b produces a Kirrel3 variant characterized by a truncated intracellular domain lacking the PDZ-binding domain typical for Kirrel3 and present in 95% of all isoforms. Despite the truncated tail, Kirrel3 isoforms with exon 20b are still capable of transcellular homophilic binding and can mediate cell-adhesion. The case of Kirrel3 exon 20b illustrates how the study of alternative splicing of synaptic receptors can directly instruct future studies. For example, it would be important to examine how Kirrel3 proteins with truncated tails alter and modulate the function of Kirrel3 isoforms with PDZ-binding domain in forming and maintaining synapses. Addressing this question would also shed new light on how neurons use PDZ-domains, a motif present in various scaffolding proteins known to organize and structure synapses.

In a similar vein, it will be important to study the function of secreted Kirrel3 isoforms that, together, constitute an estimated 4% of isoforms. Secreted Kirrel3 isoforms feature one or more Ig-domains and, thus, are predicted to undergo homophilic binding. It is possible that secreted Kirrel3 binds and sequesters transmembrane Kirrel3 variants and prevents their normal function in trans-cellular binding and signaling. Alternatively, secreted Kirrel3 could activate transmembrane Kirrel3 and trigger intracellular signals that are independent of cell-to-cell contact. Another key finding of the present study is that Kirrel3 alternatively uses several protein-coding exons (exons 6, 18, 19, and 22 in mouse) that fall on both the extracellular and intracellular sides of the protein. Other than the C-terminal PDZ-binding domain present in exon 22, the function of the other protein-coding exons remains unknown. However, it is reasonable to assume they are essential for Kirrel3 activity because mutations in the equivalent human domains are associated with disorders. Moreover, these domains first appear at critical branching points in chordate evolution. In this context, the newly discovered intracellular Kirrel3 exon encoding 30 amino acids present only in humans and other great apes is of particular interest as it could serve a synapse-related function unique to Hominidae.

References

Abrahams BS, Arking DE, Campbell DB, Mefford HC, Morrow EM, Weiss LA, Menashe I, Wadkins T, Banerjee-Basu S, Packer A (2013) SFARI gene 2.0: a community-driven knowledgebase for the autism spectrum disorders (ASDs). Mol Autism 4:36.

Altschul SF, Gish W, Miller W, Myers EW, Lipman DJ (1990) Basic local alignment search tool. J Mol Biol 215:403–410.

Banerjee-Basu S, Packer A (2010) SFARI gene: an evolving database for the autism research community. Dis Model Mech 3:133–135.

Benton MJ, Donoghue PC (2007) Paleontological evidence to date the tree of life. Mol Biol Evol 24:26–53.

Bhalla K, Luo Y, Buchan T, Beachem MA, Guzauskas GF, Ladd S, Bratcher SJ, Schroer RJ, Balsamo J, DuPont BR, Lilien J, Srivastava AK (2008) Alterations in CDH15 and KIRREL3 in patients with mild to severe intellectual disability. Am J Hum Genet 83:703–713.

Brignall AC, Raja R, Phen A, Prince JEA, Dumontier E, Cloutier JF (2018) Loss of Kirrel family members alters glomerular structure and synapse numbers in the accessory olfactory bulb. Brain Struct Funct 223:307–319.

Changeux JP, Christopoulos A (2017) Allosteric modulation as a unifying mechanism for receptor function and regulation. Diabetes Obes Metab 19 [Suppl 1]:4–21.

Chen FC, Li WH (2001) Genomic divergences between humans and other hominoids and the effective population size of the common ancestor of humans and chimpanzees. Am J Hum Genet 68:444–456.

Choi HMT, Schwarzkopf M, Fornace ME, Acharya A, Artavanis G, Stegmaier J, Cunha A, Pierce NA (2018) Third-generation in situ hybridization chain reaction: multiplexed, quantitative, sensitive, versatile, robust. Development 145:dev165753.

Corchete LA, Rojas EA, Alonso-López D, De Las Rivas J, Gutiérrez NC, Burguillo FJ (2020) Systematic comparison and assessment of RNA-seq procedures for gene expression quantitative analysis. Sci Rep 10:19737.

Davis MW, Jorgensen EM (2022) ApE, a plasmid editor: a freely available DNA manipulation and visualization program. Front Bioinform 2:818619.

De Rubeis S, et al. (2014) Synaptic, transcriptional and chromatin genes disrupted in autism. Nature 515:209–215.

Durcan PJ, Conradie JD, Van deVyver M, Myburgh KH (2014) Identification of novel Kirrel3 gene splice variants in adult human skeletal muscle. BMC Physiol 14:11.

Furlanis E, Scheiffele P (2018) Regulation of neuronal differentiation, function, and plasticity by alternative splicing. Annu Rev Cell Dev Biol 34:451–469.

Gomez AM, Traunmüller L, Scheiffele P (2021) Neurexins: molecular codes for shaping neuronal synapses. Nat Rev Neurosci 22:137–151.

Guo H, Duyzend MH, Coe BP, Baker C, Hoekzema K, Gerdts J, Turner TN, Zody MC, Beighley JS, Murali SC, Nelson BJ; University of Washington Center for Mendelian Genomics; Bamshad MJ, Nickerson DA, Bernier RA, Eichler EE (2019) Genome sequencing identifies multiple deleterious variants in autism patients with more severe phenotypes. Genet Med 21:1611–1620.

Hattori D, Millard SS, Wojtowicz WM, Zipursky SL (2008) Dscam-mediated cell recognition regulates neural circuit formation. Annu Rev Cell Dev Biol 24:597–620.

Hildebrand MS, et al. (2020) Severe childhood speech disorder: gene discovery highlights transcriptional dysregulation. Neurology 94: e2148–e2167.

Hisaoka T, Komori T, Fujimoto K, Kitamura T, Morikawa Y (2021) Comprehensive expression pattern of kin of irregular chiasm-like 3 in the adult mouse brain. Biochem Biophys Res Commun 563:66–72.

Holland ND (2005) Chordates. Curr Biol 15:R911–R914.

Iossifov I, et al. (2014) The contribution of de novo coding mutations to autism spectrum disorder. Nature 515:216–221.

Kalsner L, Twachtman-Bassett J, Tokarski K, Stanley C, Dumont-Mathieu T, Cotney J, Chamberlain S (2018) Genetic testing including targeted gene panel in a diverse clinical population of children with autism spectrum disorder: findings and implications. Mol Genet Genomic Med 6:171–185.

Keren H, Lev-Maor G, Ast G (2010) Alternative splicing and evolution: diversification, exon definition and function. Nat Rev Genet 11:345–355.

Koren E, Lev-Maor G, Ast G (2007) The emergence of alternative 3' and 5' splice site exons from constitutive exons. PLoS Comput Biol 3:e95.

Kuo RI, Tseng E, Eory L, Paton IR, Archibald AL, Burt DW (2017) Normalized long read RNA sequencing in chicken reveals transcriptome complexity similar to human. BMC Genomics 18:323.

Lara CO, Burgos CF, Silva-Grecchi T, Muñoz-Montesino C, Aguayo LG, Fuentealba J, Castro PA, Guzmán JL, Corringer PJ, Yévenes GE, Moraga-Cid G (2019) Large intracellular domain-dependent effects of positive allosteric modulators on glycine receptors. ACS Chem Neurosci 10:2551–2559.

Leblond CS, Cliquet F, Carton C, Huguet G, Mathieu A, Kergrohen T, Buratti J, Lemiere N, Cuisset L, Bienvenu T, Boland A, Deleuze JF, Stora T, Biskupstoe R, Halling J, Andorsdottir G, Billstedt E, Gillberg C, Bourgeron T (2019) Both rare and common genetic variants contribute to autism in the Faroe Islands. NPJ Genom Med 4:1.

Lein ES, et al. (2007) Genome-wide atlas of gene expression in the adult mouse brain. Nature 445:168–176.

Leshkowitz D, Kedmi M, Fried Y, Pilzer D, Keren-Shaul H, Ainbinder E, Dassa B (2022) Exploring differential exon usage via short- and long-read RNA sequencing strategies. Open Biol 12:220206.

Li J, Wang L, Guo H, Shi L, Zhang K, Tang M, Hu S, Dong S, Liu Y, Wang T, Yu P, He X, Hu Z, Zhao J, Liu C, Sun ZS, Xia K (2017) Targeted sequencing and functional analysis reveal brain-size-related genes and their networks in autism spectrum disorders. Mol Psychiatry 22:1282–1290.

Li J, Xie Y, Cornelius S, Jiang X, Sando R, Kordon SP, Pan M, Leon K, Südhof TC, Zhao M, Araç D (2020) Alternative splicing controls teneurin-latrophilin interaction and synapse specificity by a shape-shifting mechanism. Nat Commun 11:2140.

Lifschitz S, Haeusler EH, Catanho M, Miranda AB, Armas EM, Heine A, Moreira S, Tristão C (2022) Bio-strings: a relational database data-type for dealing with large biosequences. BioTech (Basel) 11:31.

Martin EA, Muralidhar S, Wang Z, Cervantes DC, Basu R, Taylor MR, Hunter J, Cutforth T, Wilke SA, Ghosh A, Williams ME (2015) The intellectual disability gene Kirrel3 regulates target-specific mossy fiber synapse development in the hippocampus. Elife 4:e09395.

Martin EA, Woodruff D, Rawson RL, Williams ME (2017) Examining hippocampal mossy fiber synapses by 3D electron microscopy in wildtype and Kirrel3 knockout mice. eNeuro 4:ENEURO.0088-17.2017.

O'Leary MA, et al. (2013) The placental mammal ancestor and the post-K-Pg radiation of placentals. Science 339:662–667.

Ortiz Zacarías NV, Lenselink EB, IJzerman AP, Handel TM, Heitman LH (2018) Intracellular receptor modulation: novel approach to target GPCRs. Trends Pharmacol Sci 39:547–559.

Ovando-Zambrano JC, Arias-Montaño JA, Boucard AA (2019) Alternative splicing event modifying ADGRL1/latrophilin-1 cytoplasmic tail promotes both opposing and dual cAMP signaling pathways. Ann N Y Acad Sci 1456:168–185.

Prince JE, Brignall AC, Cutforth T, Shen K, Cloutier JF (2013) Kirrel3 is required for the coalescence of vomeronasal sensory neuron axons into glomeruli and for male-male aggression. Development 140:2398–2408.

Ray TA, Cochran K, Kozlowski C, Wang J, Alexander G, Cady MA, Spencer WJ, Ruzycki PA, Clark BS, Laeremans A, He MX, Wang X, Park E, Hao Y, Iannaccone A, Hu G, Fedrigo O, Skiba NP, Arshavsky VY, Kay JN (2020) Comprehensive identification of mRNA isoforms reveals the diversity of neural cell-surface molecules with roles in retinal development and disease. Nat Commun 11:3328.

Roh JD, Choi SY, Cho YS, Choi TY, Park JS, Cutforth T, Chung W, Park H, Lee D, Kim MH, Lee Y, Mo S, Rhee JS, Kim H, Ko J, Choi SY, Bae YC, Shen K, Kim E, Han K (2017) Increased excitatory synaptic transmission of dentate granule neurons in mice lacking PSD-95-interacting adhesion molecule Neph2/Kirrel3 during the early postnatal period. Front Mol Neurosci 10:81.

Sakharkar MK, Chow VT, Kangueane P (2004) Distributions of exons and introns in the human genome. In Silico Biol 4:387–393.

Sanes JR, Zipursky SL (2020) Synaptic specificity, recognition molecules, and assembly of neural circuits. Cell 181:536–556.

Schoch CL, Ciufo S, Domrachev M, Hotton CL, Kannan S, Khovanskaya R, Leipe D, McVeigh R, O'Neill K, Robbertse B, Sharma S, Soussov V, Sullivan JP, Sun L, Turner S, Karsch-Mizrachi I (2020) NCBI taxonomy: a comprehensive update on curation, resources and tools. Database (Oxford) 2020:baaa062.

Schreiner D, Nguyen TM, Russo G, Heber S, Patrignani A, Ahrné E, Scheiffele P (2014) Targeted combinatorial alternative splicing generates brain region-specific repertoires of neurexins. Neuron 84:386–398.

Südhof TC (2017) Synaptic neurexin complexes: a molecular code for the logic of neural circuits. Cell 171:745–769.

Südhof TC (2021) The cell biology of synapse formation. J Cell Biol 220:e202103052.

Suñé-Pou M, Prieto-Sánchez S, Boyero-Corral S, Moreno-Castro C, El Yousfi Y, Suñé-Negre JM, Hernández-Munain C, Suñé C (2017) Targeting splicing in the treatment of human disease. Genes (Basel) 8:87.

Taylor MR, Martin EA, Sinnen B, Trilokekar R, Ranza E, Antonarakis SE, Williams ME (2020) Kirrel3-mediated synapse formation is attenuated by disease-associated missense variants. J Neurosci 40:5376–5388.

Traunmüller L, Schulz J, Ortiz R, Feng H, Furlanis E, Gomez AM, Schreiner D, Bischofberger J, Zhang C, Scheiffele P (2023) A cell-type-specific alternative splicing regulator shapes synapse properties in a trans-synaptic manner. Cell Rep 42:112173.

Treutlein B, Gokce O, Quake SR, Sudhof TC (2014) Cartography of neurexin alternative splicing mapped by single-molecule long-read mRNA sequencing. Proc Natl Acad Sci U S A 111:E1291–E1299.

Trivedi V, Choi HMT, Fraser SE, Pierce NA (2018) Multidimensional quantitative analysis of mRNA expression within intact vertebrate embryos. Development 145:dev156869.

Trotter JH, Wang CY, Zhou P, Nakahara G, Südhof TC (2023) A combinatorial code of neurexin-3 alternative splicing controls inhibitory synapses via a trans-synaptic dystroglycan signaling loop. Nat Commun 14:1771.

Wang J, Vaddadi N, Pak JS, Park Y, Quilez S, Roman CA, Dumontier E, Thornton JW, Cloutier JF, Özkan E (2021) Molecular and structural basis of olfactory sensory neuron axon coalescence by Kirrel receptors. Cell Rep 37:109940.

Wang T, et al. (2016) De novo genic mutations among a Chinese autism spectrum disorder cohort. Nat Commun 7:13316.

Wang X, Heinz BA, Qian YW, Carter JH, Gadski RA, Beavers LS, Little SP, Yang CR, Beck JP, Hao J, Schaus JM, Svensson KA, Bruns RF (2018) Intracellular binding site for a positive allosteric modulator of the dopamine D1 receptor. Mol Pharmacol 94:1232–1245.

Wang Y, Zhao Y, Bollas A, Wang Y, Au KF (2021) Nanopore sequencing technology, bioinformatics and applications. Nat Biotechnol 39:1348–1365.

Xia H, Bi J, Li Y (2006) Identification of alternative 5'/3' splice sites based on the mechanism of splice site competition. Nucleic Acids Res 34:6305–6313.

Xie Q, Xinyong G, Xianjin C, Yayu W (2013) PEI/DNA formation affects transient gene expression in suspension Chinese hamster ovary cells via a one-step transfection process. Cytotechnology 65:263–271.

Yuen RK, et al. (2016) Genome-wide characteristics of de novo mutations in autism. NPJ Genom Med 1:160271–1602710.

Zhou X, et al. (2022) Integrating de novo and inherited variants in 42,607 autism cases identifies mutations in new moderate-risk genes. Nat Genet 54:1305–1319.